Available online at www.sciencedirect.com
ScienceDirect
Journal of Power Sources 167 (2007) 58–63
JOURNAL OF POWER SOURCES
www.elsevier.com/locate/jpowsour

Short communication

Enhanced performance of a single-chamber solid oxide fuel cell with an SDC-impregnated cathode

Bo Wei [a,*], Zhe Lü [a], Xiqiang Huang [a], Minliang Liu [a], Kongfa Chen [a], Wenhui Su [a,b,c,*]

[a] *Center for Condensed Matter Science and Technology, Harbin Institute of Technology, Harbin 150080, PR China*
[b] *Department of Condensed Matter Physics, Jilin University, Changchun 130023, PR China*
[c] *International Center for Materials Physics, Chinese Academy of Sciences, Shenyang 110015, PR China*

Received 19 December 2006; received in revised form 7 February 2007; accepted 8 February 2007
Available online 21 February 2007

Abstract

The electrochemical performance of anode-supported single-chamber solid oxide fuel cells (SC-SOFCs) with and without SDC-impregnated cathodes was compared in a diluted methane–oxygen mixture. These cells were made of conventional materials including yttrium-stabilized zirconia (YSZ) thin film, a Ni + YSZ anode and a $La_{0.7}Sr_{0.3}MnO_3$ (LSM) cathode. Our results showed that the cell performance was greatly enhanced with the SDC-impregnated LSM cathode. At a furnace temperature of 750 °C, the maximum power density was as high as 404 mW cm^{-2} for a CH_4 to O_2 ratio of 2:1, which was 4.0 times higher than the cell with a pure LSM cathode (100 mW cm^{-2}). The overall polarization resistance of the impregnated cell was 1.6 Ω cm^2, which was much smaller than that of the non-impregnated one (4.2 Ω cm^2). The impregnation introduced SDC nanoparticles greatly extended the electrochemical active zone and hence greatly improved the cell performance.
© 2007 Elsevier B.V. All rights reserved.

Keywords: Single-chamber solid oxide fuel cells; Anode-supported; Ion impregnation; $La_{0.7}Sr_{0.3}MnO_3$; Electrochemical performance

1. Introduction

As compared to conventional solid oxide fuel cells (SOFCs), both the anode and cathode of single-chamber SOFCs (SC-SOFCs) are exposed to the same mixture of fuel and oxygen. This simple configuration of SC-SOFCs offers several advantages over dual-chamber cells, such as eliminating the sealing, rapid startup, improved thermal and mechanical shock resistance and stack design, etc. [1]. These characteristics make them attractive for small-scale power generation. Since the introduction of the "single-chamber" concept to SOFCs [2], the research has drawn increasing attention around the world, and the performance has been continuously improved [3–8].

For SC-SOFCs, the operating principle and actual electrode behaviors are very complex. Theoretical explanation of the operating mechanism has been proposed by Riess et al. [9]. It is considered that cell voltage is generated from the selective catalytic activity of the electrodes towards components of the fuel-oxygen mixture. Ideally, the anode is effective for both partial oxidation of fuels and electrochemical oxidation of the syngas products (H_2 and CO), whereas the cathode is only active toward oxygen electro-reduction. Obviously, the selection of suitable electrode materials with good selectivity is very important for SC-SOFCs. Ni + YSZ (yttrium-stabilized zirconia), Ni + SDC (Sm-doped ceria) or Ni + GDC (Gd-doped ceria) based cements are widely used as anode materials with satisfactory catalytic properties toward hydrocarbons. For the cathode, expensive metals (Au) [2], (La,Sr)MnO_3 (LSM) [7,10,11], mixed conductors like (La,Sr)(Co,Fe)$O_{3-\delta}$ (LSCF) [12,13], $Sm_{0.5}Sr_{0.5}CoO_{3-\delta}$ (SSC) [3,4,14] and $Ba_{0.5}Sr_{0.5}Co_{0.8}Fe_{0.2}O_{3-\delta}$ (BSCF) [5,8,15] have been investigated for SC-SOFC applications. Moreover, further modification of the cathode composition will improve cell performance. With an MnO_2 added LSM electrode, Hibino et al. obtained higher cell output than the cell with a pure LSM cathode [10]. Suzuki et al. have found that the composition of their LSCF-SDC composite cathodes could influence the open-

* Corresponding authors. Tel.: +86 451 86418420; fax: +86 461 86412828.
E-mail addresses: wavingwei@126.com (B. Wei), suwenhui@hit.edu.cn (W. Su).

0378-7753/$ – see front matter © 2007 Elsevier B.V. All rights reserved.
doi:10.1016/j.jpowsour.2007.02.017

circuit voltage (OCV) and cell output [13]. A LSCF-30 vol.% SDC composition showed the lowest overpotential. Shao et al. also have demonstrated that the BSCF-30 wt.% SDC composite cathode was more suitable than pure BSCF electrode for single-chamber operation [5]. Recently, Jiang et al. have developed an ion impregnation technique that can greatly reduce the cathode polarization resistance. At 700 °C, the $Gd_{0.2}Ce_{0.8}(NO_3)_x$ solution impregnated (La,Sr)MnO_3 cathode exhibited lower polarization resistance of 0.72 Ω cm^2 as compared to 26.4 Ω cm^2 of pure LSM electrode [16]. In this paper, an ion impregnation method was introduced to modify the LSM cathode of the anode-supported YSZ film cell that operated in a methane–oxygen mixture. The microstructure and electrochemical performance of the single cells without and with impregnated LSM cathodes are compared.

2. Experimental

Nickel oxide (NiO) powder was synthesized by the precipitation method using $Ni(NO_3)_2{\cdot}6H_2O$ (99.0%, analytical reagent, A.R.) and ammonia (25–28%, A.R.) as precipitator. The nickel hydroxide precursor was washed and calcined at 400 °C for 2 h to get the NiO powder. To prepare the anode substrate, powders of NiO, YSZ (TZ-8YS, Tosoh, Japan) and the pore-former (flour) were mixed together by ball-milling in the weight ratio of 5:5:2. Mixtures were uniaxially pressed into pellets of 13 mm in diameter, which were then sintered at 1100 °C for 2 h to improve the mechanical property of these substrates. Thin YSZ films were fabricated by slurry spin coating method [17]. The bi-layers of YSZ electrolyte and anode substrate were co-fired at 1400 °C for 4 h. Conventional cathode material, $La_{0.7}Sr_{0.3}MnO_3$, was synthesized by the modified Pechini method using $La(NO_3)_2{\cdot}6H_2O$ (99.5%, A.R.), $Sr(NO_3)_2$ (>99.5%), $Mn(NO_3)_2$ solution (49–51%, A.R.) and citric acid (99.5%, A.R.) as a complexing agent. The dry gel was calcined at 1000 °C for 2 h to obtain the final powder with desired perovskite structure, as confirmed by X-ray diffractometer (XRD, Bede D1, Cu Kα radiation). LSM powder was mixed with 6 wt.% ethyl cellulose-terpineol binder to form cathode slurry, which was coated on the surface of the YSZ film and sintered subsequently at 1100 °C for 2 h. The active areas of the circular cathodes were about 0.5 cm^2. Moreover, one of sintered cathodes was impregnated with a the solution containing 20 mol% $Sm(NO_3)_3$ (>99.5%, A.R.) and 80 mol% $Ce(NO_3)_3$ (>99.0%, A.R.). This cathode was dried and further calcined at 850 °C for 1 h, resulting in fine $Sm_{0.2}Ce_{0.8}O_{2-\delta}$ (SDC) type oxide in porous LSM matrix. The impregnated SDC oxide loading was estimated to be about 1.7 mg cm^{-2}.

For fuel cell tests, the surfaces of the anode and cathode were coated with a thin layer of silver paste (DAD-87, Shanghai Research Institute of Synthetic Resins) as the current collector and then connected with silver wires. Single cells were measured by the four-terminal technique in a flowing through quartz tube (the inner diameter is 17.5 mm). A schematic set-up for electrochemical testing is shown in Fig. 1. Measurements were carried out at a furnace temperature of 550–750 °C in a nitrogen diluted methane–oxygen mixture (total flow rate: 400 ml min^{-1}). Gas

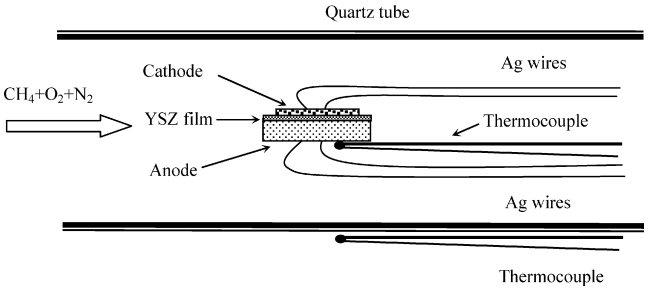

Fig. 1. Simplified schematic diagram of the measurement configuration.

composition and the CH_4 to O_2 ratio (M, changed from 1:1 to 2:1) were controlled by mass flow controllers (D08-4D/2M, Seven Star Huachuang). Since the partial oxidation of methane occurred on the anode side and is exothermic by nature, two K-type thermocouples were used to determine the difference between the furnace temperature (T_f) and the cell temperature (T_c). They were placed on the outside of the quartz tube and at the center of the anode surface (physically contacted), respectively. Polarization curves and AC impedance spectra were collected by a combined system with a Solartron SI 1287 electrochemical interface and a Solartron SI 1260 impedance grain/phase analyzer. Impedance spectra were obtained under open-circuit conditions in the frequency range of 91 kHz to 0.1 Hz with a signal amplitude of 10 mV. The microstructure of single cell and cathodes were observed by scanning electron microscope (SEM, JEOL-JSM6480LV).

3. Results and discussion

The SEM images of single cell and LSM cathodes are shown in Fig. 2. It is clear that the NiO + YSZ anode, YSZ thin film and LSM cathode (after impregnation) well adhered to each other. The YSZ membrane was uniform and dense enough with an average thickness of 8 μm. At the anode, large pores caused by the pore-former facilitate reduction of the anode and the transport of gases in the relatively thick substrate. For pure cathode (Fig. 2b) LSM particles were well-contacted after sintering at 1100 °C for 2 h and these grains were homogeneous with a particle size of about 0.3 μm. After wet impregnation (Fig. 2c), the cathode microstructure changed significantly. LSM grains were covered by many fine SDC particles and the pores were also partly filled with the porosity decreasing from about 44 to 27%. Such nano-scale ionic conducting phase greatly extended the electrochemical reaction area and consequently lowered the cathodic overpotential.

The polarization and power density curves of the cells without and with impregnation at CH_4 to O_2 ratio of 2:1 are compared in Fig. 3. These data were obtained at a furnace temperature (T_f) of 600–750 °C, and the temperatures in brackets represented the actual cell temperatures (T_c), which were higher than the furnace temperatures due to exothermic reactions. For the first cell with a pure LSM cathode (Fig. 3a), the discharge curve of 600 °C showed a strange kink, which was caused by the oscillatory behavior of the cell voltage. The maximum output of this cell was reached at a T_c of 700 °C, with the maxi-

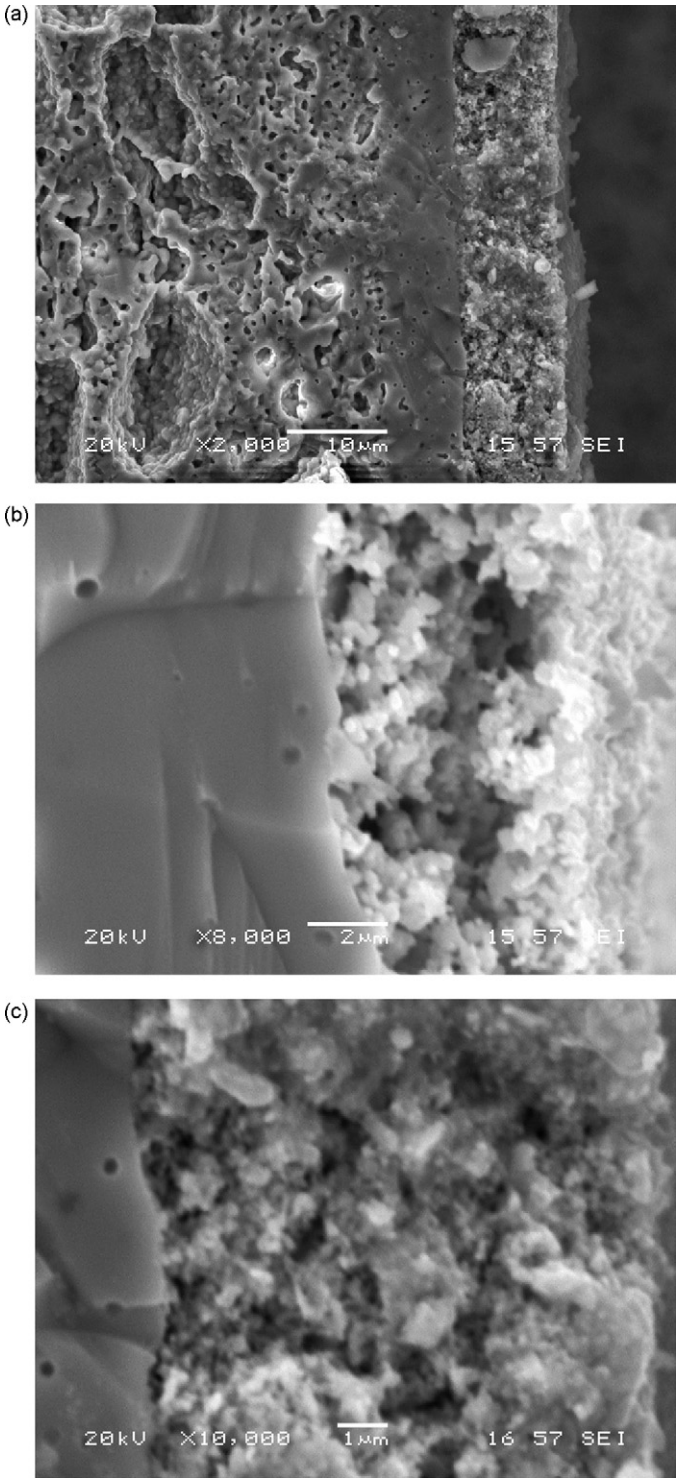

Fig. 2. Typical SEM micrographs of the cell structure: (a) cross-sectional view of the single cell, (b) pure LSM cathode and (c) SDC-impregnated LSM cathode.

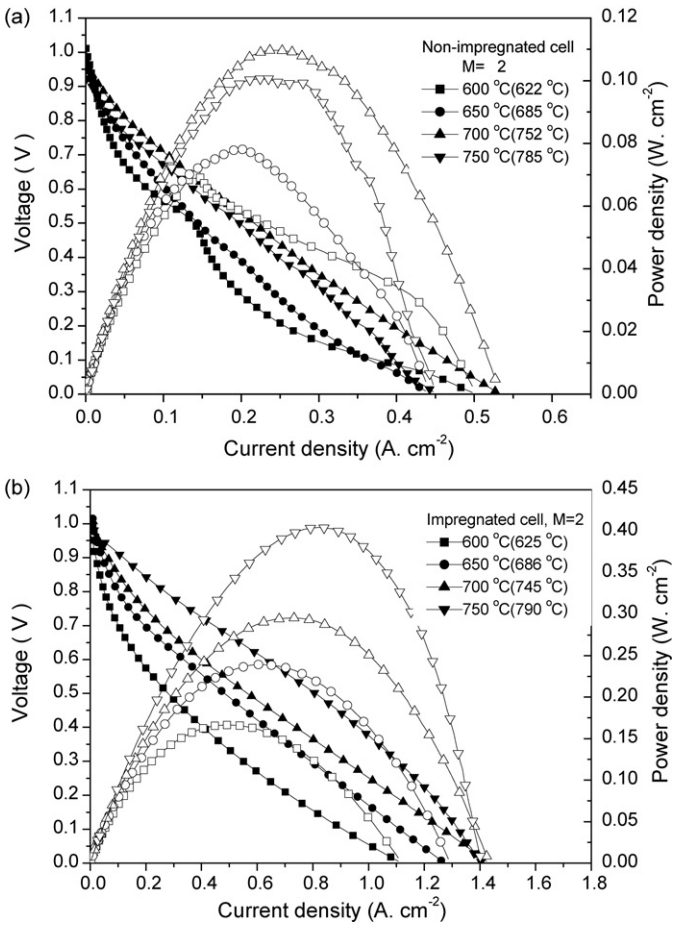

Fig. 3. The discharge and power density profiles for the cell (a) without impregnated cathode, and (b) with impregnated cathode. The performance was obtained at the furnace temperature between 600 and 750 °C with the gas composition of CH_4 = 133 ml min^{-1}, O_2 = 67 ml min^{-1} and N_2 = 200 ml min^{-1}.

mum power density (MPD) and short circuit current density of 110 mW cm^{-2} and 532 mA cm^{-2}, respectively. Such performance was comparable to an anode-supported YSZ film cell using a $La_{0.6}Sr_{0.4}Co_{0.2}Fe_{0.8}O_{3-\delta}$ (LSCF) cathode, which exhibited a MPD of 120 mW cm^{-2} at 750 °C [12]. Up to 750 °C, however, the MPD and limiting current density decreased to 100 mW cm^{-2} and 446 mA cm^{-2}. A decrease of the OCV from 0.958 to 0.924 V was also observed. For the second cell with a $Sm_{0.2}Ce_{0.8}(NO_3)_x$ impregnated LSM cathode, it exhibited a remarkable improvement as shown in Fig. 3b. At all temperatures, its output was much higher than the first cell. At 750 °C, the maximum power density and limiting current density achieved 404 mW cm^{-2} and 1404 mA cm^{-2}, which were 4.0 times and 3.2 times higher than the former cell, respectively. Note that two cells were fabricated by the same method with the only difference in the treatment procedure of the cathode, so the enhancement of performance can be ascribed to the modification of the LSM cathode. The electronic-conducting LSM network was uniformly covered by many ion-conducting SDC nanoparticles, which obviously extended the electrochemical reaction zone from the traditional electrolyte/cathode interface to the entire electrode and consequently contributed to the great improvement.

The partial oxidation of hydrocarbons to syngas (H_2 and CO) will generate a large quantity of heat, which consequently results in the heating of the cell body [18]. The cell temperatures were about 22–52 °C higher than that of the environment. Thermodynamically, the temperature rise tends to restrain the partial oxidation of methane, according to Le Chatelier's principle. But more importantly, it can greatly promote the electrochemical

oxidation of H_2 and CO. Besides, both the cathode resistance and the electrolyte resistance are further reduced, resulting in a higher performance (assuming that both electrodes work well). For the measured data, there was some difference between these two cells. At a T_f of 700 °C, for example, the measured T_c value of the non-impregnated cell was 752 °C, which was 7 °C higher than that with a modified cathode. The exothermic reactions occurring at the 650 μm thick anode should be primary source of the temperature rise, because nickel is very active toward the partial oxidation of methane. Therefore, with a similar anode substrate, the actual temperature of both cells will be very close when operated in the same condition. The difference in values may be caused by the measurement technique such as imperfect contact. The overheating temperatures measured by us were similar to the results observed by Jacques-Bedard et al. [7] for anode-supported cells with Ni + YSZ based anodes, but lower than the values obtained by Suzuki et al. (about 100 °C) [12]. Nickel-rich anodes (NiO:YSZ = 80:20 in weight) probably caused the higher overtemperature.

Impedance spectra of the cells without and with impregnated LSM cathodes are compared in Fig. 4. The spectra were fitted by Zview 2.3 software based on the equivalent circuit in Fig. 4c. In these parameters, L is the inductance, which is mainly attributed to silver voltage–current probes; R_{ohm} is the ohmic resistance including electrolyte resistance, contact resistances and electrode ohmic resistance; (R1, CPE1), (R2, CPE2) and (R3, CPE3) are corresponding to the high-, intermediate- and low-frequency arcs, respectively. It is apparent that internal resistances of the impregnated cell were significantly reduced at each measured temperature. At 750 °C, its overall resistance was about 1.6 Ω cm^2, while the resistance of the non-impregnated cell was 4.2 Ω cm^2, 2.6 times of the former. Fig. 5 shows the ohmic resistances (R_{ohm}) and electrode polarization resistances (R1 + R2 + R3) of the two cells. Clearly, electrode resistances of the untreated cell were larger than that of the modified cell. But their ohmic resistances showed a small difference between 600 and 750 °C. They were only 0.055–0.138 Ω cm^2 in the measured temperature range; the ohmic loss accounted for not more than 3.8% of the total resistance. These results indicated that the performance of these anode-supported cells was critically limited by the electrode polarization resistances. Compared with electrolyte-supported cells, the cell performance was largely limited by the electrolyte resistance which was often as much as 70–90% of the total resistance [3,4].

The OCVs of the two cells as a function of the furnace temperature and methane to oxygen ratio (M) are given in Fig. 6. At lower temperatures (600 °C), all the voltages for both cells were larger than 0.98 V. The OCVs were larger than 1.01 V when $M > 1$, which was close to the theoretical calculation based on thermodynamic equilibrium (about 1.05 V for $M = 1.5$ and 1.07 V for $M = 2$, at 600 °C) [19]. This indicated that both anode and cathode functioned with good selectivity at this temperature and the YSZ films were gas tight. With increase of the operating temperature, the OCVs for both cells tended to decrease monotonically. The drop of voltage can be mainly assigned to

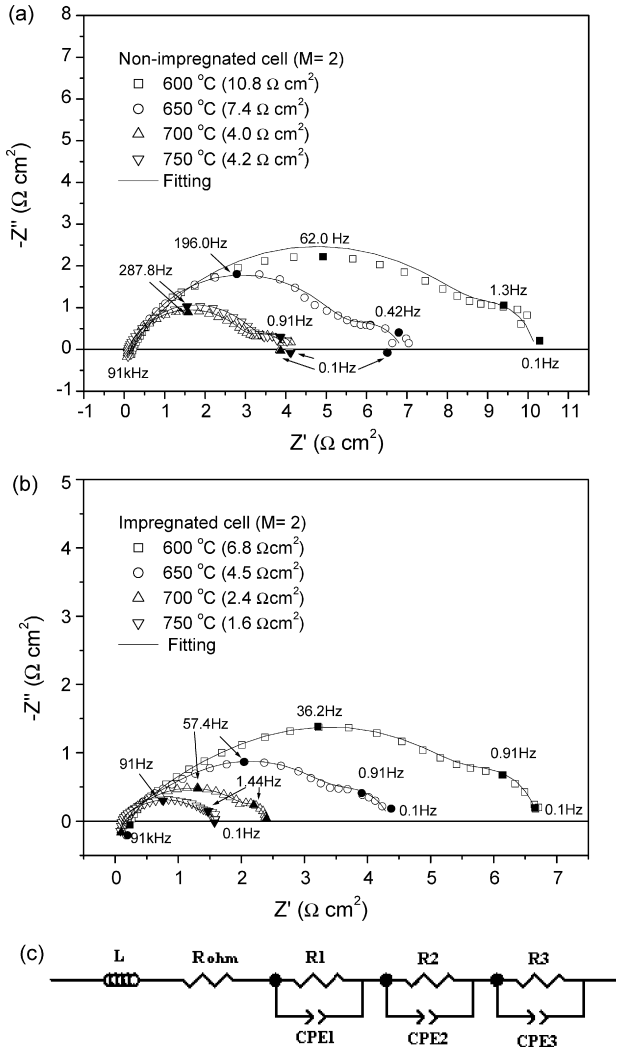

Fig. 4. Impedance spectra for (a) the cell with non-impregnated cathode, (b) the cell with impregnated cathode, (c) Equivalent circuit for data fitting. These spectra were obtained under open circuit condition between 600 and 750 °C. Total resistances were given in the brackets.

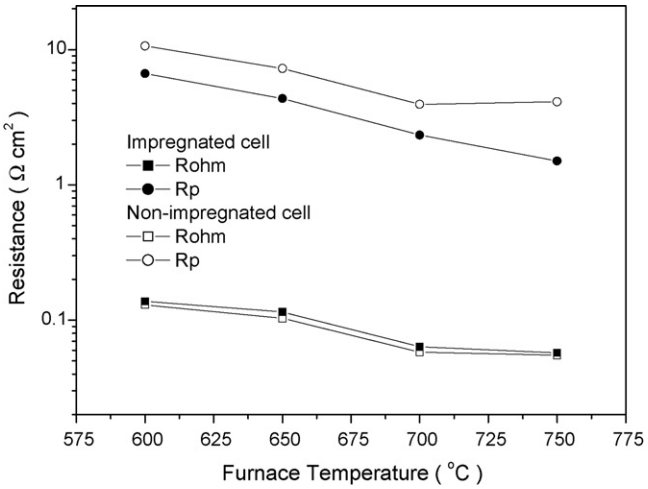

Fig. 5. Ohmic resistances (R_{ohm}) and the electrode polarization resistances (R_p) obtained from the impedance spectra.

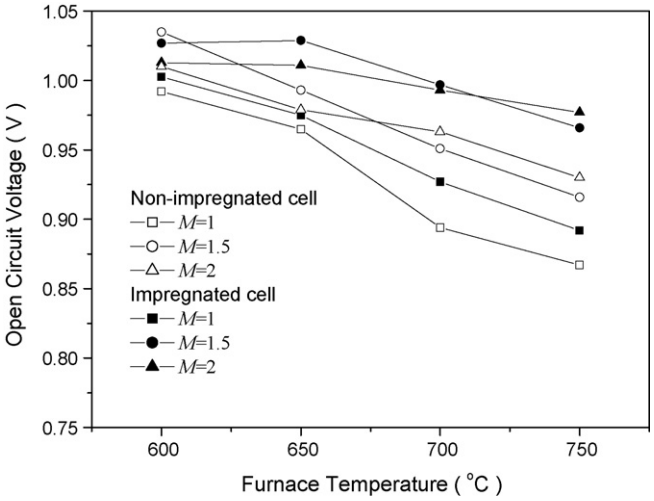

Fig. 6. Comparison of the open circuit voltage (OCV) of the cell without and with SDC-impregnated cathode.

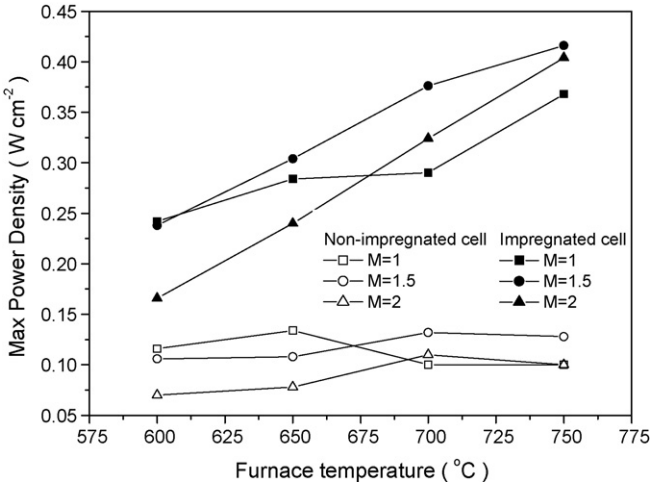

Fig. 7. Comparison of the maximum power density (MPD) of the cell without and with SDC-impregnated cathode.

the imperfect selectivity of the electrodes at elevated temperatures. Especially, LSM cathodes became catalytically active toward methane. Parasitic catalytic combustion of fuel consumed oxygen and decreased the oxygen partial pressure near the cathode, resulting in the decrease of OCV. At 700 and 750 °C, the OCVs of the modified cell were about 25–50 mV higher than the untreated cell. This indicated that the impregnated LSM electrode exhibited had improved selective catalytic activity at higher temperatures, due to the introduction of the nanosized SDC grains on the LSM surface. Fine SDC particles in the composite cathode provided more reaction sites for oxygen reduction and also functioned as the ionic conducting phase to enhance oxygen ionic conduction. In addition, it is well-known that ceria can readily store and transfer oxygen [20]. These factors weakened the catalytic reaction toward methane to some extend at higher temperature, leading to a relative higher OCV of the impregnated cell. Suzuki et al. also found that the addition of SDC to LSCF cathodes generally resulted in higher OCVs of single cells [13].

The SC-SOFC configuration also allows the use of a porous electrolyte. For example, a cell with a 18 μm YSZ film (about 23% porosity) generated an OCV of 680–780 mV and a MPD of 660 mW cm^{-2} [21]. But it is obvious that the OCVs using a porous electrolyte are lower than our cells with dense films, since the partial oxidation products (H_2 and CO) in the anode diffuse into the deeper regions towards the electrolyte. If there are some open pores in the film, they can further diffuse to the cathode side through the membrane and the OCV should be depressed. So a dense electrolyte film is still important for the SC-SOFC. With a dense gas-tight electrolyte film, higher OCVs and further improved output can be achieved.

The maximum power densities of the two cells as a function of furnace temperature and CH_4 to O_2 ratios are shown in Fig. 7. It is apparent that impregnated cell showed superior output than the un-treated cell under each measured condition. The MPD of impregnated cell increased gradually from 600 to 750 °C, but the MPD of un-treated cell changed relative less. At 750 °C and $M = 1.5$, the highest output of 416 mW cm^{-2} was achieved. At $M = 1.5$ was found the optimum ratio at 650–750 °C, which was basically consistent with the theoretical predication ($M = 1.67$) [22]. In oxygen-richer conditions ($M = 1$), the discharge profiles at 700 and 750 °C showed obvious concentration polarization in higher current density regions (data not given). Because, with increased oxygen concentration, more non-electrochemical active products (CO_2 and H_2O) are generated from the total oxidation reaction that are deleterious to the electrochemical oxidations of H_2 and CO [7].

4. Conclusion

In nitrogen-diluted methane–oxygen mixtures, a single cell with an SDC modified LSM cathode showed remarkably enhanced performance compared with a non-impregnated cell. At a temperature of 750 °C and $M = 2$, the impregnated cell exhibited a maximum power density of 404 mW cm^{-2} and a polarization resistance of 1.6 Ω cm^2 which were 4.0 times higher and 38.1% of the non-impregnated cell, respectively. The modified LSM cathode also showed improved selectivity at higher temperatures. The introduction of uniformly-distributed SDC nanoparticles in the LSM matrix contributed to the observed improvements. Consequently, our results showed that ion impregnation is a simple and effective method to improve the performance of SC-SOFCs and this technique could be also applied to other kinds of cathode materials.

Acknowledgements

This research was supported by the Ministry of Science and Technology of China (No. 2001AA323090). We greatly appreciate the kindly help from Dr. Y. Hao, Prof. D. Goodwin at California Institute of Technology, and Prof. J. Liu at South China University of Technology.

References

[1] M. Yano, A. Tomita, M. Sano, T. Hibino, Solid State Ionics 177 (2007) 3351–3359.

[2] T. Hibino, H. Iwahara, Chem. Lett. (1993) 1131–1134.
[3] T. Hibino, A. Hashimoto, T. Inoue, J. Tokuno, S. Yoshida, M. Sano, Science 288 (2000) 2031–2033.
[4] T. Hibino, A. Hashimoto, M. Yano, M. Suzuki, S. Yoshida, M. Sano, J. Electrochem. Soc. 149 (2002) A133–A136.
[5] Z.P. Shao, S.M. Haile, Nature 431 (2004) 170–173.
[6] B.E. Buergler, M.E. Siegrist, L.J. Gauckler, Solid State Ionics 176 (2005) 1717–1722.
[7] X. Jacques-Bedard, T.W. Napporn, R. Roberge, M. Meunier, J. Power Sources 153 (2006) 108–113.
[8] Z. Shao, J. Mederos, W.C. Chueh, S.M. Haile, J. Power Sources 162 (2006) 589–596.
[9] I. Riess, P.J. Vanderput, J. Schoonman, Solid State Ionics 82 (1995) 1–4.
[10] T. Hibino, S.Q. Wang, S. Kakimoto, M. Sano, Solid State Ionics 127 (2000) 89–98.
[11] T.W. Napporn, X. Jacques-Bedard, F. Morin, M. Meunier, J. Electrochem. Soc. 151 (2004) A2088–A2094.
[12] T. Suzuki, P. Jasinski, V. Petrovsky, H.U. Anderson, F. Dogan, J. Electrochem. Soc. 151 (2004) A1473–A1476.
[13] T. Suzuki, P. Jasinski, H.U. Anderson, F. Dogan, J. Electrochem. Soc. 151 (2004) A1678–A1682.
[14] Z.P. Shao, C. Kwak, S.M. Haile, Solid State Ionics 175 (2004) 39–46.
[15] Z.P. Shao, S.M. Haile, J. Ahn, P.D. Ronney, Z.L. Zhan, S.A. Barnett, Nature 435 (2005) 795–798.
[16] S.P. Jiang, Y.J. Leng, S.H. Chan, K.A. Khor, Electrochem, Solid State Lett. 6 (2003) A67–A70.
[17] K.F. Chen, Z. Lu, N. Ai, X.Q. Huang, Y.H. Zhang, X.S. Xin, R.B. Zhu, W.H. Su, J. Power Sources 160 (2006) 436–438.
[18] T. Hibino, A. Hashimoto, T. Inoue, J. Tokuno, S. Yoshida, M. Sano, J. Electrochem. Soc. 148 (2001) A544–A549.
[19] B.E. Buergler, A.N. Grundy, L.J. Gauckler, J. Electrochem. Soc. 153 (2006) A1378–A1385.
[20] C.E. Hori, H. Permana, K.Y.S. Ng, A. Brenner, K. More, K.M. Rahmoeller, D. Belton, Appl. Catal. B Environ. 16 (1998) 105–117.
[21] T. Suzuki, P. Jasinski, V. Petrovsky, H.U. Anderson, F. Dogan, J. Electrochem. Soc. 152 (2005) A527–A531.
[22] Y. Hao, D.G. Goodwin, J. Electrochem. Soc. 154 (2007) B207–B217.